Quantum Tunneling in Peroxide O−O Bond Breaking Reaction

Yangyu Zhou,[§] Wei Fang,[§] Lina Wang, Xiaoqing Zeng,* Dong H. Zhang,* and Mingfei Zhou*

Cite This: *J. Am. Chem. Soc.* 2023, 145, 8817−8821

Read Online

ACCESS | 📊 Metrics & More | 📖 Article Recommendations | 🆂🅸 Supporting Information

ABSTRACT: The importance of quantum-mechanical tunneling becomes increasingly recognized in chemical reactions involving hydrogen as well as heavier atoms. Here we report concerted heavy-atom tunneling in an oxygen−oxygen bond breaking reaction from cyclic beryllium peroxide to linear dioxide in cryogenic Ne matrix, as evidenced by subtle temperature-dependent reaction kinetics and unusually large kinetic isotope effects. Furthermore, we demonstrate that the tunneling rate can be tuned through noble gas atom coordination on the electrophilic beryllium center of $Be(O_2)$, as the half-life dramatically increased from 0.1 h for $NeBe(O_2)$ at 3 K to 12.8 h for $ArBe(O_2)$. Quantum chemistry and instanton theory calculations reveal that noble gas coordination notably stabilizes the reactants and transition states, increases the barrier heights and widths, and consequently reduces the reaction rate drastically. The calculated rates and in particular kinetic isotope effects are in good agreement with experiment.

In the classical picture, a chemical reaction with an energetic barrier can only proceed at reaction energies higher than the barrier, leading to the well-known Arrhenius formula for reaction rates. However, chemical reactions can occur at energies below the reaction barrier through quantum-mechanical tunneling (QMT), resulting in the deviation of the reaction rates from the Arrhenius behavior and unusually large kinetic isotope effects (KIEs).[1−4] The effect of QMT becomes especially important in low-temperature environments such as the interstellar medium.[5,6] Since the first introduction of QMT in chemistry,[7−9] QMT has been recognized to play important roles in a variety of light hydrogen-atom transfer reactions.[10−14]

Aside from the apparent mass effect, quantum tunneling is also strongly dependent on the height and width of the reaction barrier. The possibility of heavy-atom tunneling in reactions with narrow yet high barriers was first emphasized by Wigner[8] and was demonstrated by the automerization of cyclobutadiene with concerted motion of the endocyclic carbon and hydrogen atoms in the four-membered ring.[15] Later on, more and more tunneling reactions by carbon have been observed for diverse organic systems in the low-temperature processes.[16−23] QMT involving nitrogen atom has been reported for the spin crossover isomerization of transient nitrene intermediates in noble gas matrices.[24−26] Theoretical studies reveal that the barriers are cusped through spin crossover, leading to significantly reduced barrier widths to allow heavy-atom tunneling.[27] Recent reports show that quantum tunneling also contributes to the rotation of carbon monoxide adsorbed on condensed surfaces.[28−30] Here we report a clear-cut example of concerted heavy-atom tunneling by oxygen and beryllium atoms during the spin crossover ring-opening reaction of singlet beryllium peroxide to form triplet linear dioxide in cryogenic Ne matrix.

The beryllium−oxygen species are generated via the reactions of beryllium atoms with dioxygen in solid neon and are detected by infrared absorption spectroscopy, as described in detail in Supporting Information. Two absorptions at 1310.4 and 1064.1 cm^{-1} are produced upon $\lambda < 280$ nm UV light irradiation (Figure S1), which spontaneously convert into a 1431.4 cm^{-1} absorption when the sample is left in the dark at 3 K (Figure S2). Based on the isotopic shift and splitting (Figure S3), the 1310.4 and 1064.1 cm^{-1} absorptions can be assigned to a cyclic $Be(O_2)$ species. The 1431.4 cm^{-1} absorption is attributed to the linear beryllium dioxide isomer. The cyclic $Be(O_2)$ molecule was predicted to have a singlet ($^1A_1$) ground state with C_{2v} symmetry.[31−33] The Be center has an atomic charge of +1.36.[33] The lowest unoccupied molecular orbital is primarily a hybrid of Be 2s and 2p atomic orbitals that is directed away from the oxygen atom (Figure S4). These indicate that the Be center in $Be(O_2)$ is highly electrophilic, analogous to the diatomic BeO molecule, which is the strongest diatomic Lewis acid that binds rather strongly with a noble gas atom.[34,35] Thus, the cyclic $Be(O_2)$ molecule trapped in solid neon may in fact coordinated by a neon atom, and the 1310.4 and 1064.1 cm^{-1} absorptions should be assigned to the $NeBe(O_2)$ complex rather than the bare $Be(O_2)$ molecule.

The assignment of $NeBe(O_2)$ is confirmed by argon doping experiments. As shown in Figure 1, an additional red-shifted absorption is produced for each mode of $NeBe(O_2)$ when 0.25% argon is doped into neon. These newly appearing absorptions are due to the $ArBe(O_2)$ complex formed by replacing the coordinated neon atom in $NeBe(O_2)$ with the heavier argon atom. In contrast, the 1431.4 cm^{-1} absorption attributed to the beryllium dioxide molecule shows very small red shift (<0.5 cm^{-1}) in the argon doping experiment (Figure
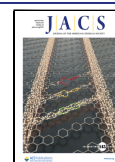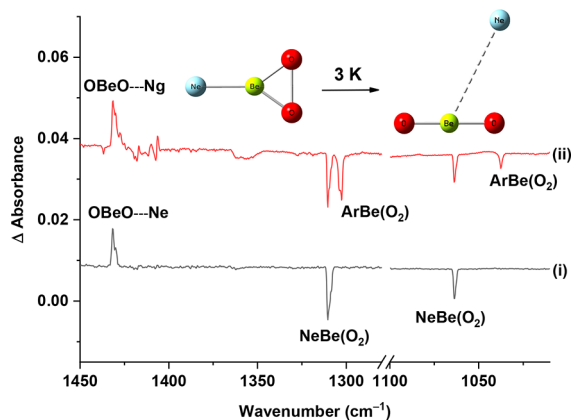
Figure 1. Difference IR spectra from codeposition of laser-evaporated Be atoms with 0.05% O_2 in neon (spectrum taken after 10 min of UV light irradiation and standing in dark for a period of time (t) minus spectrum taken right after 10 min of UV light irradiation): (i) no doping, t = 73 min; (ii) doped with 0.25% Ar, t = 46 h.

1), indicating that OBeO only forms weakly bound van der Waals complexes with the noble gas atoms (hereafter noted as OBeO···Ng).

The observation of spontaneous ring-opening reaction from the noble gas atom-coordinated beryllium peroxide complex NeBe(O_2) to the dioxide complex OBeO···Ne in solid neon suggests that the reaction takes place via QMT. The kinetics of this oxygen−oxygen bond breaking reaction are studied by monitoring the intensity changes of the IR bands of NgBe(O_2) and OBeO···Ng with time. Figure 2A shows representative difference IR spectra obtained using an equimolar mixture of $^{16}O_2$ and $^{18}O_2$. The downward absorptions represent the depletion of the NeBe($^{16}O_2$) and NeBe($^{18}O_2$) isotopologues with time, whereas the upward absorptions represent the production of the $^{16}OBe^{16}O$···Ne and $^{18}OBe^{18}O$···Ne isotopologues with time. From these experiments, the time dependences of the concentrations of the reactant and product at different temperatures are obtained (Figures S6−S15). Figure 2B shows the measured decays for the ring-opening of the NeBe($^{16}O_2$) and NeBe($^{18}O_2$) isotopologues in solid neon matrix at 3 K. Fitting the experimental data with first-order exponential decay equations gives rate constants of 1.8×10^{-3} and 3.5×10^{-4} s^{-1} for the two isotopologues, respectively, resulting in a quite large KIE of 5.1, significantly larger than the values (<1.1) reported in typical oxygen-involving reactions.[36] The half-life of NeBe($^{16}O_2$) is determined to be 6.4 min (0.1 h) at 3 K. The experimentally determined rate constants for NeBe(O_2) at different temperatures up to 8 K in solid neon are listed in Table 1, which show very small increases upon raising the temperature to 8 K. The observed subtle temperature-dependent reaction kinetics and unusually large kinetic isotope effects for the ^{18}O substitutions provide solid evidence for the occurrence of QMT in this oxygen−oxygen bond breaking reaction. The rate constant of ArBe(O_2) is determined to be 1.5×10^{-5} s^{-1}, which corresponds to a half-life of 12.8 h (Table 1). The decay rate is reduced by 120 times when the neon atom in NeBe(O_2) is replaced by argon.

Quantum chemistry calculations confirm that the cyclic beryllium peroxide molecule can be coordinated by a noble gas atom in forming the NgBe(O_2) complexes (Ng = Ne, Ar). The geometries optimized at the CCSD(T)/aug-cc-pVTZ and NEVPT2/aug-cc-pVTZ levels are very similar, as shown in
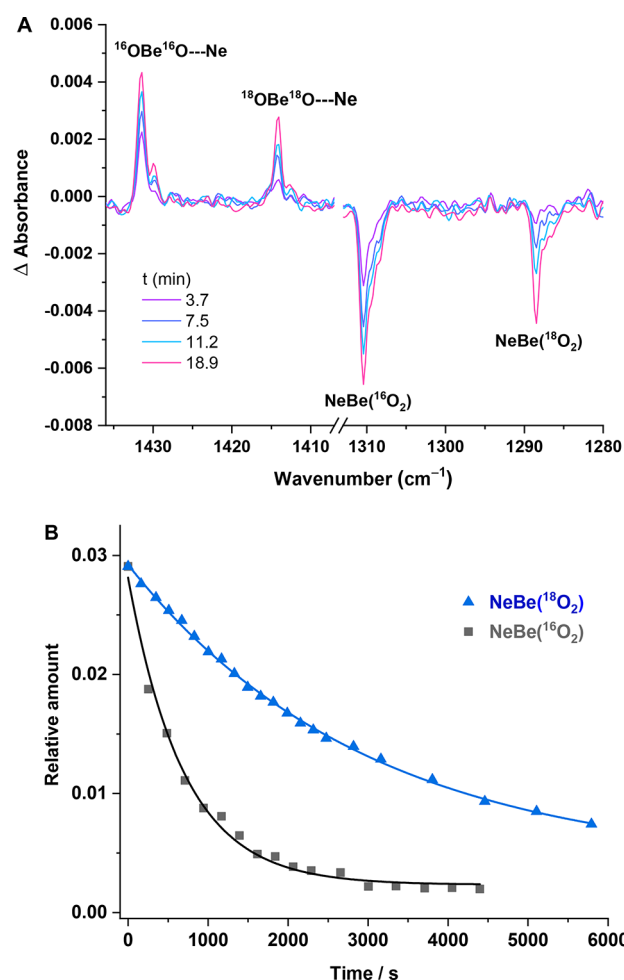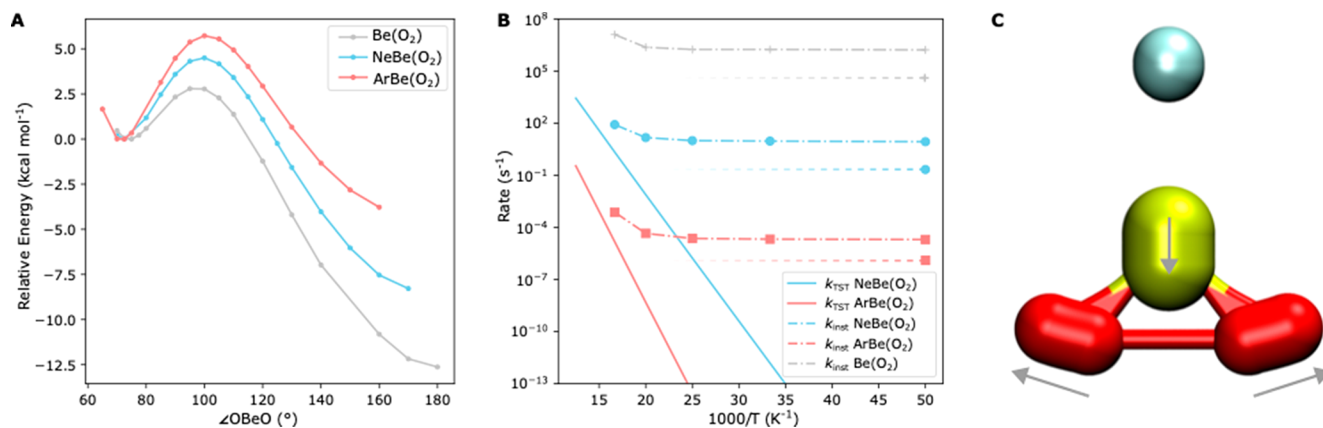

Figure 2. Observed kinetics of the NeBe(O_2) → OBeO···Ne isomerization reaction. (A) Difference IR spectra from the reaction of laser-evaporated Be atoms with 0.05% $^{16}O_2$ + 0.05% $^{18}O_2$ in neon at 3 K (spectrum taken after 10 min of UV light irradiation and standing in dark for a period of time (t) minus spectrum taken right after 10 min of UV light irradiation). (B) Kinetics of spontaneous consumption of NeBe($^{16}O_2$) and NeBe($^{18}O_2$) in neon matrix at 3 K. The solid lines represent the best fits obtained using a first-order exponential decay equation.

Figure S16. The calculations indicate that the two Be−O bond lengths become longer whereas the O−O bond becomes shorter upon noble gas atom coordination. The Ng−Be bond dissociation energies (BDEs) are predicted to be 3.6 and 9.0 kcal mol^{-1} for Ne and Ar, respectively, at the CCSD(T) level. The MRCI-F12+Q/aug-cc-pVTZ calculations give very similar values (Table S2). Bonding analyses indicate that the noble gas atom serves as an electron donor. The electron density transfer from Ng to the Be(O_2) fragment strengthens the O−O bond and weakens the bonding interactions between Be^{2+} and O_2^{2-} due to reduced electrostatic interaction (Table S3). The more stable linear beryllium dioxide isomer is predicted to have a triplet ground state ($^3\Sigma_g^-$), with an open-shell singlet state ($^1\Delta_g$) lying slightly higher in energy as reported previously.[32] The linear OBeO molecule only forms weakly bound van der Waals complexes with noble gas atoms in both the triplet and open-shell singlet states.

The potential energy profiles of these ring-opening reactions as a function of the O−Be−O bond angle were calculated at the MRCI-F12+Q level (shown in Figure 3A) to obtain the

Table 1. Experimental and Calculated Rate Constants and Half-Lives of the NgBe(O$_2$) → OBeO···Ng (Ng = Ne, Ar) Isomerization Reactions

		exptl			calcd		
species	T (K)	k (^{16}O$_2$, s^{-1})	$t_{1/2}$	k (^{18}O$_2$, s^{-1})	k (^{16}O$_2$, s^{-1})	$t_{1/2}$	k (^{18}O$_2$, s^{-1})
Be(O$_2$)					4.1×10^4	1.7×10^{-5} s	
NeBe(O$_2$)	3	1.8×10^{-3}	6.4 min	3.5×10^{-4}	2.2×10^{-1}	3.2 s	3.5×10^{-2}
	4	1.7×10^{-3}	6.8 min	3.3×10^{-4}			
	5	1.7×10^{-3}	6.8 min				
	6	2.0×10^{-3}	5.8 min				
	7	2.5×10^{-3}	4.6 min				
	8	2.7×10^{-3}	4.3 min				
ArBe(O$_2$)	3	1.5×10^{-5}	12.8 h		1.2×10^{-6}	160.5 h	

Figure 3. (A) Calculated potential energy profiles of the singlet state as a function of the O−Be−O bond angle (θ) connecting the reactants and the products. (B) Calculated rate constants based on the transition state theory (k_{TST}) and the instanton theory (k_{inst}) at the NEVPT2 level shown as Arrhenius plots. The dashed lines mark the MRCI corrected rates. (C) Optimized instanton (minimum-action tunneling pathway) for NeBe(O$_2$) at 20 K. The arrows indicate the moving directions of the tunneling atoms. The coloring of the atoms is the same as in Figure 1.

classical isomerization reaction barriers. Since the reactant has a singlet ground state whereas the product has a triplet ground state, the reaction proceeds via spin crossing. As shown in Figure S17, the crossing between the singlet and triplet states occurs after the transition state and lies lower in energy than the reactant for both systems. Thus, the barrier heights for breaking the oxygen−oxygen bond of the NgBe(O$_2$) complexes are not affected by the spin crossover. The predicted barrier heights at the NEVPT2 and MRCI-F12+Q levels are listed in Table S5. The bare Be(O$_2$) complex needs to overcome an energy barrier of about 2.8 kcal mol^{-1} to form the more stable linear OBeO isomer in the $^1\Delta_g$ state, which is slightly larger than that calculated earlier at the MRCI+Q level.[33] Noble gas atom coordination stabilizes the reactant as well as the transition state with respect to the product, as OBeO only forms weakly bound van der Waals complexes with noble gas atoms. As shown in Figure S18, the Ng−Be bond distance of the transition state is longer than that of the reactant for both reactions. This indicates that noble gas coordination would cause a steady increase of the reaction barrier, which is predicted to be 4.5 and 5.7 kcal mol^{-1} at the MRCI-F12-Q level for Ng = Ne and Ar, respectively (Table S5).

Ring−polymer instanton theory was used to calculate the tunneling rate constants and the kinetic isotope effects.[37,38] The crossover temperatures to quantum tunneling are ∼65 K for both NeBe(O$_2$) and ArBe(O$_2$). Therefore, instanton rate constants from 20−60 K were calculated at the NEVPT2 level with the assistance of Gaussian process regression and

corrected at the MRCI-F12+Q level (shown in Figure 3B). At 3 K, the calculated rate constants based on the transition state theory are over 200 orders of magnitude smaller than the experimental values, indicating that the contribution from passage over the barrier is negligible and the tunneling contribution dominates. In contrast, the rate constants based on the instanton theory become temperature-independent below 40 K. As shown in Table 1, the instanton theory calculations predict that the reaction rate is reduced by about 5 orders of magnitude upon neon atom coordination on Be(O$_2$). An additional 5 orders of magnitude reduction is predicted when the neon atom in NeBe(O$_2$) is replaced by an argon atom. Apart from the apparent increase of the barrier height, noble gas coordination also notably enhances the barrier width (Table S5) and consequently reduces the tunneling rate. The predicted rates are in reasonable agreement with the experimental values considering that the calculations are based on the gas-phase free molecules whereas the experimental values are measured in solid neon matrix, which apparently will affect the tunneling rate as discussed previously.[17,20] The ArBe(O$_2$) complex in solid argon matrix decays with a rate of 6.4×10^{-6} s^{-1} at 3 K, about 2 times slower than that in neon. The KIE (^{16}O$_2$/^{18}O$_2$) of NeBe(O$_2$) reaction at 3 K is predicted to be 6.2, in good agreement with the experimental value of 5.1. The optimal tunneling pathways (Figure 3C) reveal a concerted tunneling mechanism of oxygen and Be, where the two oxygen atoms contribute about 84% of the squared mass-weighted tunneling path length and the remainder is from the metal atom (Be). While corner-

cutting effects are modest in this reaction, they do play a key role in minimizing the unfavorable tunneling of the Ng atom in the optimal tunneling path.

The present finding shows that the beryllium peroxide oxygen−oxygen bond breaking reaction is dominated by QMT. It is conceivable that QMT plays an important role in other oxygen−oxygen bond breaking or forming reactions. Previous theoretical studies already predicted that the barrier for the ring-opening isomerization reaction of the elusive cyclic ozone can be penetrated by facile oxygen tunneling.[39] Our results also show that the tunneling rates can be fine-tuned via noble gas atom coordination, which may serve as a practical strategy of controlling the tunneling reactions involving an electrophilic metal center.

■ ASSOCIATED CONTENT

Ⓢ Supporting Information

The Supporting Information is available free of charge at https://pubs.acs.org/doi/10.1021/jacs.3c02750.

Experimental and theoretical details, IR spectral assignment, bonding analysis, benchmark against MRCI, MRCI correction to instanton rates, $^{16}O/^{18}O$ kinetic isotope effect, spin crossover, additional experimental infrared spectra, kinetics of $NgBe(O_2)$ to OBeO at different temperatures, and calculated vibrational frequencies and geometries (PDF)

■ AUTHOR INFORMATION

Corresponding Authors

Xiaoqing Zeng − *Department of Chemistry, Collaborative Innovation Center of Chemistry for Energy Materials, Shanghai Key Laboratory of Molecular Catalysis and Innovative Materials, Fudan University, Shanghai 200438, China;* ⓞ orcid.org/0000-0003-4611-2094; Email: xqzeng@fudan.edu.cn

Dong H. Zhang − *Department of Chemistry, Collaborative Innovation Center of Chemistry for Energy Materials, Shanghai Key Laboratory of Molecular Catalysis and Innovative Materials, Fudan University, Shanghai 200438, China; State Key Laboratory of Molecular Reaction Dynamics, Dalian Institute of Chemical Physics, Chinese Academy of Sciences, Dalian 116023, China;* ⓞ orcid.org/0000-0001-9426-8822; Email: zhangdh@dicp.ac.cn

Mingfei Zhou − *Department of Chemistry, Collaborative Innovation Center of Chemistry for Energy Materials, Shanghai Key Laboratory of Molecular Catalysis and Innovative Materials, Fudan University, Shanghai 200438, China;* ⓞ orcid.org/0000-0002-1915-6203; Email: mfzhou@fudan.edu.cn

Authors

Yangyu Zhou − *Department of Chemistry, Collaborative Innovation Center of Chemistry for Energy Materials, Shanghai Key Laboratory of Molecular Catalysis and Innovative Materials, Fudan University, Shanghai 200438, China*

Wei Fang − *Department of Chemistry, Collaborative Innovation Center of Chemistry for Energy Materials, Shanghai Key Laboratory of Molecular Catalysis and Innovative Materials, Fudan University, Shanghai 200438, China*

Lina Wang − *Department of Chemistry, Collaborative Innovation Center of Chemistry for Energy Materials, Shanghai Key Laboratory of Molecular Catalysis and Innovative Materials, Fudan University, Shanghai 200438, China*

Complete contact information is available at:
https://pubs.acs.org/10.1021/jacs.3c02750

Author Contributions

§Y.Z. and W.F. contributed equally.

Notes

The authors declare no competing financial interest.

■ REFERENCES

(1) Borden, W. T. Reactions that involve tunneling by carbon and the role that calculations have played in their study. *Wiley Interdiscip. Rev.: Comput. Mol. Sci.* **2016**, *6*, 20−46.

(2) Meisner, J.; Kästner, J. Atom tunneling in chemistry. *Angew. Chem., Int. Ed.* **2016**, *55*, 5400−5413.

(3) Schreiner, P. R. Tunneling control of chemical reactions: The third reactivity paradigm. *J. Am. Chem. Soc.* **2017**, *139*, 15276−15283.

(4) Schreiner, P. R. Quantum mechanical tunneling is essential to understanding chemical reactivity. *Trends Chem.* **2020**, *2*, 980−989.

(5) Hiraoka, K.; Sato, T.; Takayama, T. Tunneling reactions in interstellar ices. *Science* **2001**, *292*, 869−870.

(6) Shannon, R. J.; Blitz, M. A.; Goddard, A.; Heard, D. E. Accelerated chemistry in the reaction between the hydroxyl radical and methanol at interstellar temperatures facilitated by tunnelling. *Nat. Chem.* **2013**, *5*, 745−749.

(7) Hund, F. Zur deutung der molekelspektren. III. *Z. Phys.* **1927**, *43*, 805−826.

(8) Wigner, E. Über das Überschreiten von potentialschwellen bei chemischen reaktionen. *Z. Phys. Chem.* **1932**, *19B*, 203−216.

(9) Bell, R. P. The application of quantum mechanics to chemical kinetics. *Proc. R. Soc. London, Ser. A* **1933**, *139*, 466−474.

(10) Cha, Y.; Murray, C. J.; Klinman, J. P. Hydrogen tunneling in enzyme reactions. *Science* **1989**, *243*, 1325−1330.

(11) Kohen, A.; Cannio, R.; Bartolucci, S.; Klinman, J. P. Enzyme dynamics and hydrogen tunnelling in a thermophilic alcohol dehydrogenase. *Nature* **1999**, *399*, 496−499.

(12) Schreiner, P. R.; Reisenauer, H. P.; Pickard, F. C., IV; Simmonett, A. C.; Allen, W. D.; Mátyus, E.; Császár, A. G. Capture of hydroxymethylene and its fast disappearance through tunnelling. *Nature* **2008**, *453*, 906−909.

(13) Schreiner, P. R.; Reisenauer, H. P.; Ley, D.; Gerbig, D.; Wu, C. H.; Allen, W. D. Methylhydroxycarbene: Tunneling control of a chemical reaction. *Science* **2011**, *332*, 1300−1303.

(14) Richardson, J. O.; Pérez, C.; Lobsiger, S.; Reid, A. A.; Temelso, B.; Shields, G. C.; Kisiel, Z.; Wales, D. J.; Pate, B. H.; Althorpe, S. C. Concerted hydrogen-bond breaking by quantum tunneling in the water hexamer prism. *Science* **2016**, *351*, 1310−1313.

(15) Carpenter, B. K. Heavy-atom tunneling as the dominant pathway in a solution-phase reaction? Bond shift in antiaromatic annulenes. *J. Am. Chem. Soc.* **1983**, *105*, 1700−1701.

(16) Schleif, T.; Prado Merini, M.; Sander, W. The mystery of the benzene-oxide/oxepin equilibrium—Heavy-atom tunneling reversed by solvent interactions. *Angew. Chem., Int. Ed.* **2020**, *59*, 20318−20322.

(17) Schleif, T.; Prado Merini, M.; Henkel, S.; Sander, W. Solvation effects on quantum tunneling reactions. *Acc. Chem. Res.* **2022**, *55*, 2180−2190.

(18) Michel, C. S.; Lampkin, P. P.; Shezaf, J. Z.; Moll, J. F.; Castro, C.; Karney, W. L. Tunneling by 16 carbons: Planar bond shifting in [16]annulene. *J. Am. Chem. Soc.* **2019**, *141*, 5286−5293.

(19) Castro, C.; Karney, W. L. Heavy-atom tunneling in organic reactions. *Angew. Chem., Int. Ed.* **2020**, *59*, 8355−8366.

(20) Zuev, P. S.; Sheridan, R. S.; Albu, T. V.; Truhlar, D. G.; Hrovat, D. A.; Borden, W. T. Carbon tunneling from a single quantum state. *Science* **2003**, *299*, 867−870.

(21) Greer, E. M.; Cosgriff, C. V.; Doubleday, C. Computational evidence for heavy-atom tunneling in the Bergman cyclization of a 10-membered-ring enediyne. *J. Am. Chem. Soc.* **2013**, *135*, 10194−10197.

(22) Stolz, S.; Gröning, O.; Prinz, J.; Brune, H.; Widmer, R. Molecular motor crossing the frontier of classical to quantum tunneling motion. *Proc. Natl. Acad. Sci. U.S.A.* **2020**, *117*, 14838−14842.

(23) Bernhardt, B.; Schauermann, M.; Solel, E.; Eckhardt, A. K.; Schreiner, P. R. Equilibrating parent aminomercaptocarbene and CO_2 with 2-amino-2-thioxoacetic acid via heavy-atom quantum tunnel. *Chem. Sci.* **2022**, *14*, 130−135.

(24) Wu, Z.; Feng, R.; Li, H.; Xu, J.; Deng, G.; Abe, M.; Bégué, D.; Liu, K.; Zeng, X. Fast heavy-atom tunneling in trifluoroacetyl nitrene. *Angew. Chem., Int. Ed.* **2017**, *56*, 15672−15676.

(25) Nunes, C. M.; Knezz, S. N.; Reva, I.; Fausto, R.; McMahon, R. J. Evidence of a nitrene tunneling reaction: Spontaneous rearrangement of 2-formyl phenylnitrene to an imino ketene in low-temperature matrixes. *J. Am. Chem. Soc.* **2016**, *138*, 15287−15290.

(26) Nunes, C. M.; Eckhardt, A. K.; Reva, I.; Fausto, R.; Schreiner, P. R. Competitive nitrogen versus carbon tunneling. *J. Am. Chem. Soc.* **2019**, *141*, 14340−14348.

(27) Heller, E. R.; Richardson, J. O. Heavy-atom quantum tunnelling in spin crossovers of nitrenes. *Angew. Chem., Int. Ed.* **2022**, *61*, No. e202206314.

(28) Choudhury, A.; DeVine, J. A.; Sinha, S.; Lau, J. A.; Kandratsenka, A.; Schwarzer, D.; Saalfrank, P.; Wodtke, A. M. Condensed-phase isomerization through tunnelling gateways. *Nature* **2022**, *612*, 691−695.

(29) Lau, J. A.; Choudhury, A.; Li, C.; Schwarzer, D.; Verma, V. B.; Wodtke, A. M. Observation of an isomerizing double-well quantum system in the condensed phase. *Science* **2020**, *367*, 175−178.

(30) Heinrich, A. J.; Lutz, C. P.; Gupta, J. A.; Eigler, D. M. Molecule cascades. *Science* **2002**, *298*, 1381−1387.

(31) Thompson, C. A.; Andrews, L. Reactions of laser-ablated Be atoms with O_2-Infrared spectra of beryllium oxides in solid argon. *J. Chem. Phys.* **1994**, *100*, 8689−8699.

(32) Zhang, Q. N.; Jerabek, P.; Chen, M. H.; Zhou, M. F.; Frenking, G. The oxygen-rich beryllium oxides BeO_4 and BeO_6. *Angew. Chem., Int. Ed.* **2016**, *55*, 10863−10867.

(33) Ariyarathna, I. R.; Miliordos, E. The versatile personality of beryllium: $Be(O_2)_{1−2}$ vs $Be(CO)_{1−2}$. *J. Phys. Chem. A* **2017**, *121*, 7051−7058.

(34) Frenking, G.; Koch, W.; Reichel, F.; Cremer, D. Light noble gas chemistry-Structures, stabilities, and bonding of helium, neon and argon compounds. *J. Am. Chem. Soc.* **1990**, *112*, 4240−4256.

(35) Thompson, C. A.; Andrews, L. Noble gas complexes with BeO: Infrared spectra of Ng-BeO (Ng = Ar, Kr, Xe). *J. Am. Chem. Soc.* **1994**, *116*, 423−424.

(36) Howe, G. W.; van der Donk, W. A. ^{18}O kinetic isotope effects reveal an associative transition state for phosphite dehydrogenase catalyzed phosphoryl transfer. *J. Am. Chem. Soc.* **2018**, *140*, 17820−17824.

(37) Kästner, J. Theory and simulation of atom tunneling in chemical reactions. *Wiley Interdiscip. Rev.: Comput. Mol. Sci.* **2014**, *4*, 158−168.

(38) Richardson, J. O. Ring-polymer instanton theory. *Int. Rev. Phys. Chem.* **2018**, *37*, 171−216.

(39) Chen, J. L.; Hu, W.-P. Theoretical prediction on the thermal stability of cyclic ozone and strong oxygen tunneling. *J. Am. Chem. Soc.* **2011**, *133*, 16045−16053.

📖 Recommended by ACS